Propagation of Light Beam through Lens-Like Media with Complex Permittivity

SHINNOSUKE SAWA, MEMBER, IEEE

Abstract—**Primary characteristics of the light beam propagation through a complex-permittivity lens-like medium are investigated in more detail than in previous papers, with the help of approximate wave theory. Explicit general expressions for the spot size and the curvature of the phase front of a Gaussian beam as well as the real-valued ray transfer matrix are derived, and detailed numerical investigations are presented. The existence of a new type of propagation, in which the light beam propagates with constant amplitude of undulation, neither converging nor diverging, is pointed out. Furthermore, precise conditions are given for the occurence of convergent, divergent, and critical propagation, and the corresponding profiles of the real and imaginary parts of the complex permittivity in the transverse cross section are illustrated. The results of this paper will be useful for the evaluation of the effects of loss distributions inherent in practical optical fibers consisting of lens-like media, and also for the analysis or synthesis of laser resonators or amplifiers including a loss or gain distribution.**

I. INTRODUCTION

THE DEVELOPMENT of optical fibers has made remarkable progress. Roughly speaking, we have two types of optical fibers, graded index fibers [1] and step index fibers [2].

The present paper discusses the propagation behaviors of the light beam along optical fibers consisting of a lens-like medium (graded index) with a loss or gain variation in the transverse cross section. The lens-like medium of this kind may be called, "complex-permittivity lens-like medium," because of its complex-valued dielectric constant. The complex-permittivity lens-like medium has already been analyzed by several authors [3]–[6]. They reported that the complex-permittivity lens-like medium has some interesting properties which do not appear in the lens-like medium without a loss or gain variation, a so-called real-valued permittivity lens-like medium. For example, the light beam with off-axis incident conditions converges undulatingly towards the center axis of the medium as it propagates, when the gain is highest on axis, while it diverges and wanders away from the center axis when the gain is lowest on axis. The previous works [3]–[6], however, do not provide rigorous criteria for the convergent and divergent propagation behavior of the light beam. Further, those analyses [3]–[6] put emphasis on the convergent propagation rather than the divergent one, and hence especially numerical investigations of the divergent propagation appear to be insufficient. Furthermore, the ray transfer matrix obtained so far [6] is that with complex components (a complex-valued ray transfer matrix), so that it is not straightforward to infer the results of analysis from the matrix by inspection, and it would be inconvenient for considering various applications of the medium to optical circuits.

In the present paper, fundamental characteristics of the light beam propagating along straight and circularly bent sections of the lens-like medium with complex permittivity are studied in more detail than in the previous papers [3]–[6], by making use of a convenient method of analysis devised previously [3], [7]. For simplicity and to emphasize the essential points of the argument, we use a two-dimentional lens-like medium and limit the analysis to the paraxial approximations throughout the paper. Explicit general expressions for the spot size and the curvature of the phase front of a Gaussian beam as well as the real-valued ray transfer matrix (the matrix with real components) are derived, and numerical investigations of the theoretical results are presented. It is also pointed out that there exists a new type of propagation of the light beam, the critical propagation, in which the light beam propagates with a constant amplitude of undulation, neither converging nor diverging. Moreover, the precise conditions for the convergent, divergent, and critical propagations to occur are derived, and the corresponding profiles of the real and imaginary parts of the complex permittivity in the transverse cross section are illustrated.

II. PERMITTIVITY PROFILE AND WAVE EQUATION

We consider a two-dimensional model of the complex-permittivity lens-like medium as shown in Fig. 1. Let the permittivity of the medium in the straight section be

$$\epsilon(x) = \epsilon_r - G_r^2 x^2 - j(\epsilon_i - G_i^2 x^2) \tag{1}$$

where $\epsilon_r - j\epsilon_i$ is a complex constant and x is the distance from the center axis of the medium (optic axis). G_r^2 and G_i^2 measure the degree of the variation of the complex permittivity $\epsilon(x)$.

The real part of (1), Re $\{\epsilon(x)\} = \epsilon_r - G_r^2 x^2$, repre-

Manuscript received November 25, 1974; revised February 19, 1975.

The author is with the Department of Electronics, Faculty of Engineering, Ehime University, Bunkyo Machi 3, Matsuyama City, 790 Japan.

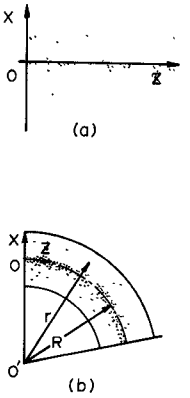

Fig. 1. Straight and circularly bent sections of the lens-like medium with complex permittivity. (a) Straight section in which permittivity $\epsilon(x)$ is given by (1). (b) Circularly bent section in which permittivity $\epsilon(r)$ is represented as $\epsilon(r) = \epsilon_r - G_r^2(r - R)^2 - j[\epsilon_i - G_i^2(r - R)^2]$ with $r = x + R$.

sents the profile of the effective dielectric constant, while the imaginary part of (1), Im $\{\epsilon(x)\} = -(\epsilon_i - G_i^2x^2)$, denotes the profile of the net loss or gain, according to $\epsilon_i - G_i^2x^2 > 0$ or $\epsilon_i - G_i^2x^2 < 0$.

Fig. 2 illustrates such profiles in the transverse x direction. For example, Fig. 2(a) represents the case for $\epsilon_i = G_i^2 = 0$, in which the permittivity of the medium is given by the real-valued $\epsilon(x) = \epsilon_r - G_r^2x^2$. Fig. 2(d) denotes the case for $\epsilon_i > 0$ and $G_i^2 = 0$, in which the net loss is uniformly distributed in the transverse cross section of the lens-like medium whose effective dielectric constant is the same as in Fig. 2(a). Fig. 2(e) shows the cases that the net loss takes the highest value on axis and decreases quadratically with the distance x in the cross section of the same lens-like medium as shown in Fig. 2(a).

For the convenience of the following analysis, we rewrite (1) in the form

$$\epsilon(x) = \epsilon(0)(1 - g^2x^2) \tag{2}$$

with

$$\epsilon(0) = \epsilon_r - j\epsilon_i \tag{3}$$

$$g = g_r - jg_i. \tag{4}$$

The parameters used in (3) and (4) are given below

$$g_r = \left[\frac{1}{2}\left(\frac{[(\epsilon_r^2 + \epsilon_i^2)(G_r^4 + G_i^4)]^{1/2} + \epsilon_iG_r^2 + \epsilon_rG_i^2}{\epsilon_r^2 + \epsilon_i^2}\right)\right]^{1/2} \tag{5}$$

$$g_i = \pm\left[\frac{1}{2}\left(\frac{[(\epsilon_r^2 + \epsilon_i^2)(G_r^4 + G_i^4)]^{1/2} - \epsilon_rG_r^2 - \epsilon_iG_i^2}{\epsilon_r^2 + \epsilon_i^2}\right)\right]^{1/2} \tag{6}$$

where $g_r > 0$ is assumed, and hence the upper and lower signs in (6) correspond to the cases of $\epsilon_rG_i^2 \geq \epsilon_iG_r^2$ and $\epsilon_rG_i^2 < \epsilon_iG_r^2$, respectively.

The response of the electromagnetic fields of light beams

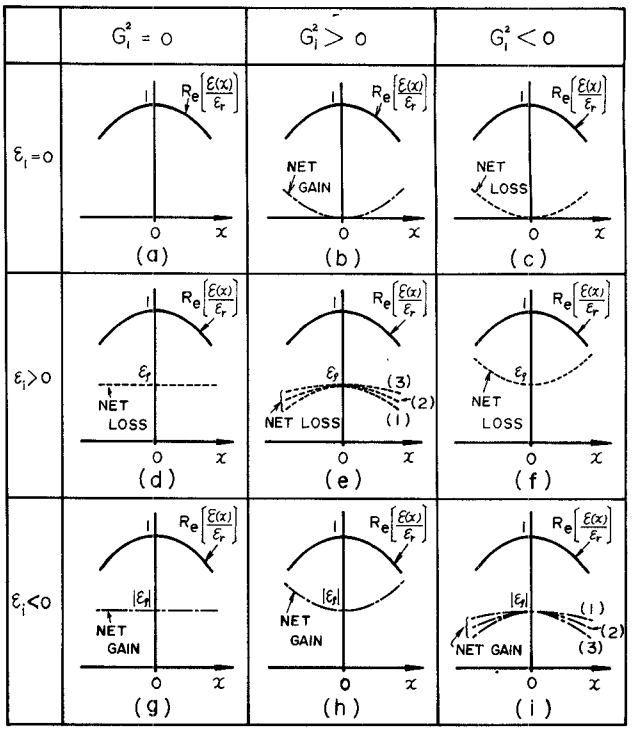

Fig. 2. Illustrations of the profiles of the effective permittivity Re $[\epsilon(x)/\epsilon_r]$ (real part of $\epsilon(x)/\epsilon_r$) and the net loss or gain Im $[\epsilon(x)/\epsilon_r]$ (imaginary part of $\epsilon(x)/\epsilon_r$) in the transverse cross section of the complex-permittivity lens-like medium. It is assumed that the curves in (e) and (i) correspond to the cases (1) $\epsilon_rG_r^2 > \epsilon_iG_r^2$, (2) $\epsilon_rG_i^2 = \epsilon_iG_r^2$ and (3) $\epsilon_rG_i^2 < \epsilon_iG_r^2$, respectively, and also that $\epsilon_r > 0$ and $G_r^2 > 0$ ($\epsilon_\rho \equiv \epsilon_i/\epsilon_r$).

propagating along the medium with the permittivity given in the form (2) can be approximately determined from the wave equation

$$\frac{\partial^2V}{\partial x^2} + \frac{\partial^2V}{\partial z^2} + k^2(0)(1 - g^2x^2)V = 0 \tag{7}$$

where

$$k(0) = \omega[\mu\epsilon(0)]^{1/2} \equiv k_r - jk_i \tag{8}$$

with

$$k_r = \omega(\mu\epsilon_r)^{1/2}\{[(1 + \epsilon_i^2/\epsilon_r^2)^{1/2} + 1]/2\}^{1/2}, \quad (> 0) \tag{9}$$

$$k_i = \pm\omega(\mu\epsilon_r)^{1/2}\{[(1 + \epsilon_i^2/\epsilon_r^2)^{1/2} - 1]/2\}^{1/2}, \quad (\epsilon_i \gtrless 0). \tag{10}$$

In the foregoing equations, sinusoidal time dependence of the fields with angular frequency ω is assumed and μ denotes the permeability of the medium [3], [7].

If we put

$$V(x,z) = U(x,z)\exp[-jk(0)z] \tag{11}$$

with the assumption

$$\left|\frac{\partial^2U}{\partial z^2}\right| \ll 2\,|\,k(0)\,|\,\left|\frac{\partial U}{\partial z}\right| \tag{12}$$

and substitute this into (7), we find that the field distribution function $U(x,z)$ satisfies the paraxial wave equation

$$\frac{\partial^2 U}{\partial x^2} - j2k(0)\frac{\partial U}{\partial z} - k^2(0)g^2x^2U = 0 \tag{13}$$

which determines the response of the electromagnetic fields of the light beams along the straight section.

In a similar fashion, we obtain the corresponding wave equation in the circularly bent section as shown in Fig. 1(b) as follows

$$\frac{\partial^2 \tilde{U}}{\partial x^2} - j2k(0)\frac{\partial \tilde{U}}{\partial z} - k^2(0)\left(-\frac{2}{R}x + \tilde{g}^2x^2\right)\tilde{U} = 0 \tag{14}$$

where

$$\tilde{g} = g(1 - 2/g^2R^2)^{1/2} \equiv \tilde{g}_r - j\tilde{g}_i \tag{15}$$

with the parameters

$$\tilde{g}_r = g_r\lambda^+ + g_i\lambda^-, \qquad \tilde{g}_i = g_i\lambda^+ - g_r\lambda^-$$

$$\lambda^{\pm} = \left(\frac{1}{2}\left\{\left[1 - \frac{4}{|g|^4R^2}\left(g_r^2 - g_i^2 - \frac{1}{R^2}\right)\right]^{1/2} \pm 1 + \frac{2(g_r^2 - g_i^2)}{|g|^4R^2}\right\}\right)^{1/2}. \tag{16}$$

In the above expression, R represents the radius of curvature of the circular bend.

III. BEHAVIORS OF LIGHT BEAMS

A. Behaviors in a Straight Section

An important first step to clarify the behavior of the light beams along the medium whose permittivity is given by (2) is to analyze the propagation of a Hermite Gaussian wave. Thus we assume that incident beam at $z = 0$ is expressed as a Hermite Gaussian beam having input wavefront coefficient[1] $1/S^2(0)$ together with the input slope $\delta'(0)$ and the input displacement $\delta(0)$ of the beam center from the optic axis $x = 0$. Then, the field distribution function $U(x,z)$ is determined from (13), according to the convenient method of analysis [3], [7], as shown in the Appendix. As a result, the primary parameters, i.e., the propagation constant of the normal modes in the straight section γ_n, the wavefront coefficient[1] $1/S^2(z)$, the trajectory of the beam center $\delta(z)$, and its slope $\delta'(z)$ are derived as follows:

[1] The wavefront coefficient $1/S^2(z)$ used in the present paper is a complex parameter to characterize a Gaussian beam, and is defined with the spot size $w(z)$ and the radius of phase front curvature $R(z)$ of a Gaussian beam as

$$\frac{1}{S^2(z)} = \frac{1}{w^2(z)} + j\frac{k_r}{R(z)}.$$

This parameter can also be related to the well-known complex beam parameter $1/q(z)$ [11] as

$$\frac{1}{S^2(z)} = j\frac{k_r}{q(z)}.$$

$$\gamma_n = j\{k_r - jk_i - (n + \tfrac{1}{2})(g_r - jg_i)\} \tag{17}$$

$$\frac{1}{S^2(z)} = \frac{1}{S^2(0)}\left(\frac{\cos gz - j[S^2(0)/\Omega^2]\sin gz}{\cos gz - j[\Omega^2/S^2(0)]\sin gz}\right) \tag{18}$$

$$\begin{bmatrix}\delta(z)\\ \delta'(z)\end{bmatrix} = \begin{bmatrix}T_{11} & T_{12}\\ T_{21} & T_{22}\end{bmatrix}\begin{bmatrix}\delta(0)\\ \delta'(0)\end{bmatrix} \tag{19}$$

where $1/\Omega^2(=gk(0))$ is the characteristic wavefront coefficient, and n denotes the mode numbers of the normal modes. $[T_{ij}]$ is the real-valued ray transfer matrix, unlike the complex-valued one obtained so far [6]. The components of the real-valued ray transfer matrix $[T_{ij}]$ are real and given below

$$\begin{aligned}T_{11} = {} & [\{K_a - K_b(g_\rho - 1/\Omega_\rho^2)u(z)\}\cosh g_iz \\ & + \{K_au(z) - K_b(g_\rho - v(z))\}\sinh g_iz]\cos g_rz \\ & - [\{K_b(1 + g_\rho v(z)) - K_au(z)/\Omega_\rho^2\}\cosh g_iz \\ & + \{K_b(1 + g_\rho/\Omega_\rho^2)u(z) - K_av(z)\}\sinh g_iz]\sin g_rz\end{aligned} \tag{20a}$$

$$\begin{aligned}T_{12} = {} & (1/g_r\Theta)[[[\{1 + g_\rho v(z) - K_cu(z)/\Omega_\rho^2\}\cosh g_iz \\ & + \{u(z)(1 + g_\rho/\Omega_\rho^2) - K_cv(z)\}\sinh g_iz]\sin g_rz \\ & + [\{(g_\rho - 1/\Omega_\rho^2)u(z) - K_c\}\cosh g_iz \\ & + \{g_\rho - v(z) - K_cu(z)\}\sinh g_iz]\cos g_rz]]\end{aligned} \tag{20b}$$

$$\begin{aligned}T_{21} = {} & g_r[[[\{K_a(g_\rho + 1/\Omega_\rho^2)u(z) - K_b(1 + g_\rho^2) \\ & - K_b(g_\rho - 1/\Omega_\rho^2)u'(z)\}\cosh g_iz \\ & + \{K_a(g_\rho + v(z)) - K_b(1 + g_\rho^2)u(z) + K_au'(z) \\ & + K_bv'(z)\}\sinh g_iz]\cos g_rz \\ & - [\{K_a[1 - g_\rho v(z)] + K_b(1 + g_\rho^2)u(z)/\Omega_\rho^2 \\ & - K_au'(z)/\Omega_\rho^2 + K_bg_\rho v'(z)\}\cosh g_iz \\ & + \{K_a(1 - g_\rho/\Omega_\rho^2)u(z) + K_b(1 + g_\rho^2)v(z) \\ & - K_av'(z) + K_bu'(z)(1 + g_\rho/\Omega_\rho^2)\}\sinh g_iz]\sin g_rz]]\end{aligned} \tag{20c}$$

$$\begin{aligned}T_{22} = {} & (1/\Theta)[[[\{(1 + g_\rho^2)v(z) + K_c(1 - g_\rho/\Omega_\rho^2)u(z) \\ & + (1 + g_\rho/\Omega_\rho^2)u'(z) - K_cv'(z)\}\sinh g_iz \\ & + \{(1 + g_\rho^2)u(z)/\Omega_\rho^2 + K_c(1 - g_\rho v(z)) \\ & + g_\rho v'(z) - K_cu'(z)/\Omega_\rho^2\}\cosh g_iz]\sin g_rz \\ & + [\{(1 + g_\rho^2)u(z) - K_c(g_\rho + v(z)) - K_cu'(z) \\ & - v'(z)\}\sinh g_iz + \{1 + g_\rho^2 - K_c(g_\rho + 1/\Omega_\rho^2)u(z) \\ & + (g_\rho - 1/\Omega_\rho^2)u'(z)\}\cosh g_iz]\cos g_rz]]\end{aligned} \tag{20d}$$

in which

$$\begin{aligned}K_a &= 1 + s_r^4(g_\rho^2 - 1/\Omega_\rho^4)/\Theta \\ K_b &= s_r^2(g_\rho + 1/\Omega_\rho^2)/\Theta \\ K_c &= s_r^2(g_\rho - 1/\Omega_\rho^2)\end{aligned} \tag{21a}$$

$$\Theta = 1 + g_\rho^2 - \frac{2K_c}{1+\Omega_\rho^4}\left\{\frac{g_\rho + \Omega_\rho^2}{s_i^2} - \frac{\Omega_\rho^2(1-g_\rho\Omega_\rho^2)}{2s_r^2}\left(1 - \frac{s_r^4}{\Omega_\rho^4 s_i^4}\right)\right\} \quad (21b)$$

$$u(z) = \frac{p_1 \cosh 2g_i z - p_3 \sinh 2g_i z + p_2 \cos 2g_r z - \Omega_\rho^2 p_4 \sin 2g_r z}{p_3 \cosh 2g_i z - p_1 \sinh 2g_i z - p_4 \cos 2g_r z - (p_2/\Omega_\rho^2)\sin 2g_r z}$$

$$v(z) = \frac{(1/\Omega_\rho^2)(p_3 \cosh 2g_i z - p_1 \sinh 2g_i z) + \Omega_\rho^2 p_4 \cos 2g_r z + p_2 \sin 2g_r z}{p_3 \cosh 2g_i z - p_1 \sinh 2g_i z - p_4 \cos 2g_r z - (p_2/\Omega_\rho^2)\sin 2g_r z}$$

$$u'(z) = \frac{1}{g_r}\frac{du(z)}{dz}, \qquad v'(z) = \frac{1}{g_r}\frac{dv(z)}{dz}. \quad (21c)$$

In (20a)–(20d) and (21a)–(21c), the parameters g_ρ, Ω_ρ, s_r, s_i, and p_j ($j = 1,2,3,4$) are represented as

$$g_\rho = g_i/g_r, \qquad \Omega_\rho = \left(\mathrm{Re}\left\{\frac{1}{\Omega^2}\right\} \Big/ \mathrm{Im}\left\{\frac{-1}{\Omega^2}\right\}\right)^{1/2}$$

$$s_r = \left(\mathrm{Re}\left\{\frac{1}{\Omega^2}\right\} \Big/ \mathrm{Re}\left\{\frac{1}{S^2(0)}\right\}\right)^{1/2}$$

$$s_i = \left(\mathrm{Im}\left\{\frac{1}{\Omega^2}\right\} \Big/ \mathrm{Im}\left\{\frac{1}{S^2(0)}\right\}\right)^{1/2}$$

$$p_1 = 1 + \frac{1}{s_i^4} + \Omega_\rho^4\left(1 + \frac{1}{s_r^4}\right)$$

$$p_2 = 1 - \frac{1}{s_i^4} + \Omega_\rho^4\left(1 - \frac{1}{s_r^4}\right)$$

$$p_3 = 2\left(\frac{\Omega_\rho^4}{s_r^2} + \frac{1}{s_i^2}\right) \qquad p_4 = 2\left(\frac{1}{s_i^2} - \frac{1}{s_r^2}\right). \quad (22)$$

Moreover, the expressions for the spot size $w(z)$ and the curvature of the phase front $1/R(z)$ of the Gaussian beam are obtained, respectively, as

$$w(z) = \left(u(z) \Big/ \mathrm{Re}\left\{\frac{1}{\Omega^2}\right\}\right)^{1/2} \quad (23)$$

$$\frac{1}{R(z)} = \frac{-v(z)}{k_r u(z)}\mathrm{Re}\left\{\frac{1}{\Omega^2}\right\}. \quad (24)$$

For the special case that $1/S^2(0) = 1/\Omega^2$, we have the simplified results for $\delta(z)$, $\delta'(z)$, $w(z)$, and $1/R(z)$ as follows:

$$\begin{bmatrix}\delta(z)\\ \delta'(z)\end{bmatrix} = \exp(g_i z)\begin{bmatrix}\cos g_r z - (g_i/g_r)\sin g_r z & (1/g_r)\sin g_r z\\ -g_r(1 + g_i^2/g_r^2)\sin g_r z & \cos g_r z + (g_i/g_r)\sin g_r z\end{bmatrix}\begin{bmatrix}\delta(0)\\ \delta'(0)\end{bmatrix} \quad (25)$$

$$w(z) = \left(\mathrm{Re}\left\{\frac{1}{\Omega^2}\right\}\right)^{-1/2} \equiv w_0 \quad (26)$$

$$\frac{1}{R(z)} = \frac{1}{k_r}\cdot \mathrm{Im}\left\{\frac{1}{\Omega^2}\right\} \equiv \frac{1}{R_0}. \quad (27)$$

B. Behaviors in a Circular Bend

The behaviors of a light beam in a circular bend as shown in Fig. 1(b) can be described in a similar manner as in the straight section. The result of the analysis yields the response of a Hermite Gaussian wave beam with the same incidence conditions as in the straight section as follows: the wavefront coefficient $1/\tilde{S}^2(z)$, the trajectory of the beam center $\tilde{\delta}(z)$, and its slope $\tilde{\delta}'(z)$ are obtained as

$$\frac{1}{\tilde{S}^2(z)} = \frac{1}{S^2(0)}\left(\frac{\cos \tilde{g}z - j[S^2(0)/\tilde{\Omega}^2]\sin \tilde{g}z}{\cos \tilde{g}z - j[\tilde{\Omega}^2/S^2(0)]\sin \tilde{g}z}\right) \quad (28)$$

$$\begin{bmatrix}\tilde{\delta}(z) - \tilde{\delta}_c(z)\\ \tilde{\delta}'(z) - \tilde{\delta}_c'(z)\end{bmatrix} = \begin{bmatrix}\tilde{T}_{11} & \tilde{T}_{12}\\ \tilde{T}_{21} & \tilde{T}_{22}\end{bmatrix}\begin{bmatrix}\delta(0)\\ \delta'(0) - \tilde{\delta}_c'(0)\end{bmatrix} \quad (29)$$

where

$$\begin{aligned}\tilde{\delta}_c(z) = \frac{1}{\tilde{g}_r^2(1+\tilde{g}_\rho^2)R}[[\{1 - \tilde{g}_\rho^2 + 2\tilde{g}_\rho\tilde{v}(z)\}\\ \cdot(1 - \cosh \tilde{g}_i z \cos \tilde{g}_r z)\\ - \tilde{u}(z)(1 - \tilde{g}_\rho^2 + 2\tilde{g}_\rho/\tilde{\Omega}_\rho^2)\sinh \tilde{g}_i z \cos \tilde{g}_r z\\ - [\tilde{u}(z)\{2\tilde{g}_\rho - (1 - \tilde{g}_\rho^2)/\tilde{\Omega}_\rho^2\}\cosh \tilde{g}_i z\\ + \{2\tilde{g}_\rho - \tilde{v}(z)(1 - \tilde{g}_\rho^2)\}\sinh \tilde{g}_i z]\sin \tilde{g}_r z]] \end{aligned} \quad (30)$$

and

$$\tilde{\delta}_c'(z) = \frac{d}{dz}\tilde{\delta}_c(z). \quad (31)$$

In (30), the parameters $\tilde{g}_\rho$, $\tilde{\Omega}_\rho$, $\tilde{u}(z)$, and $\tilde{v}(z)$ are obtained from (21a)–(21c) and (22) by replacing all the parameters g_r and g_i in those expressions by $\tilde{g}_r$ and $\tilde{g}_i$ given in (16), respectively. The components of the real-valued ray transfer matrix $[\tilde{T}_{ij}]$ are also obtained from (20a)–(20d) and (21a)–(21c) with the same procedure.

Furthermore, the spot size $\tilde{w}(z)$ and the curvature of the phase front $1/\tilde{R}(z)$ of the Gaussian beam are derived from (23) and (24) by replacing all the parameters $u(z)$, $v(z)$, and $1/\Omega^2$ in those expressions by $\tilde{u}(z)$, $\tilde{v}(z)$, and

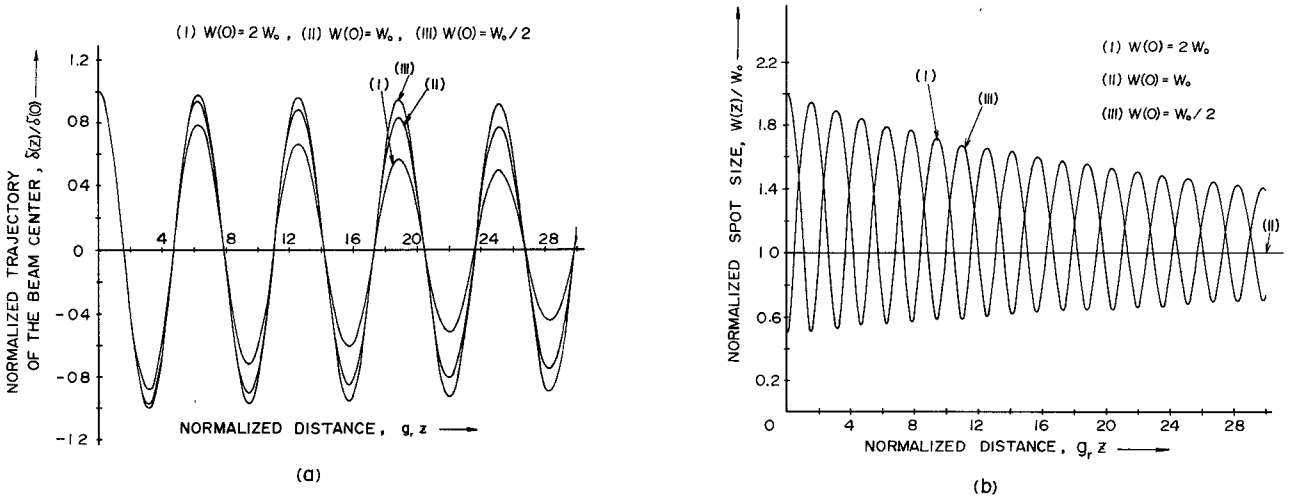

Fig. 3. Propagation behaviors of the convergent light beam guided along the straight section. (a) Normalized trajectory of the beam center. (b) Normalized spot size. ($g_i/g_r = -0.01$, $\epsilon_i/\epsilon_r = 10^{-3}$, $\delta'(0) = 0$, $R(0) = R_0$.)

$1/\tilde{\Omega}^2$, respectively, where $1/\tilde{\Omega}^2$ represents the characteristic wavefront coefficient in the circularly bent section.

Consider the special case that the light beam with the matched input wavefront coefficient $1/S^2(0) = 1/\tilde{\Omega}^2$ is incident upon the circularly bent section. In this case, the expressions for $\tilde{\delta}(z)$, $\tilde{\delta}'(z)$, $\tilde{w}(z)$, and $1/\tilde{R}(z)$ are simplified to

$$\tilde{\delta}(z) = \exp(\tilde{g}_i z)\left[\left(\cos\tilde{g}_r z - \frac{\tilde{g}_i}{\tilde{g}_r}\sin\tilde{g}_r z\right)\{\delta(0) - \delta_c\} + \frac{\delta'(0)}{\tilde{g}_r}\sin\tilde{g}_r z\right] + \delta_c \quad (32)$$

$$\tilde{\delta}'(z) = \exp(\tilde{g}_i z)\left[-\{\delta(0) - \delta_c\}\tilde{g}_r\left(1 + \frac{\tilde{g}_i^2}{\tilde{g}_r^2}\right)\sin\tilde{g}_r z + \delta'(0)\left(\cos\tilde{g}_r z + \frac{\tilde{g}_i}{\tilde{g}_r}\sin\tilde{g}_r z\right)\right] \quad (33)$$

$$\tilde{w}(z) = \left(\mathrm{Re}\left[\frac{1}{\tilde{\Omega}^2}\right]\right)^{-1/2} \equiv \tilde{w}_0 \quad (34)$$

$$\frac{1}{\tilde{R}(z)} = \frac{1}{k_r}\cdot\mathrm{Im}\left\{\frac{1}{\tilde{\Omega}^2}\right\} \equiv \frac{1}{\tilde{R}_0} \quad (35)$$

where

$$\delta_c = \frac{1 - \tilde{g}_\rho^2 + 2\tilde{g}_\rho/\tilde{\Omega}_\rho^2}{\tilde{g}_r^2(1 + \tilde{g}_\rho^2)R}. \quad (36)$$

C. Numerical Examples and Discussions

According to the theoretical results obtained in the preceding sections, let us illustrate numerically the propagation behaviors of the Gaussian beam in the straight and circularly bent sections. Figs. 3–6 show the calculated trajectories of the beam center $\delta(z)$ and $\tilde{\delta}(z)$ normalized by the input value $\delta(0)$, and the calculated spot sizes $w(z)$ and $\tilde{w}(z)$ normalized by the characteristic spot sizes w_0 and $\tilde{w}_0$, as a function of the normalized distance z/g_r^{-1} or $z/\tilde{g}_r^{-1}$. The medium constants g_i/g_r, $\tilde{g}_i/\tilde{g}_r$, ϵ_i/ϵ_r, and $1/\tilde{g}_r R$ and the input conditions of the light beam, the values of $\delta(0)$, $\delta'(0)$, $w(0)$, $\tilde{w}(0)$, $R(0)$, and $\tilde{R}(0)$ used for the numerical calculations are given in these figures. The curves (I), (II), and (III) correspond to the cases that $w(0) = 2w_0$, $w(0) = w_0$, and $w(0) = w_0/2$ in the straight section, and $w(0) = 2\tilde{w}_0$, $w(0) = \tilde{w}_0$, and $w(0) = \tilde{w}_0/2$ in the circularly bent section, respectively, where $w(0)$ is the input spot size. Figs. 3 and 5 illustrate examples of the convergent propagation for the cases of g_i/g_r, $\tilde{g}_i/\tilde{g}_r = -10^{-2}$, and Figs. 4 and 6, those of the divergent propagation for the cases of g_i/g_r, $\tilde{g}_i/\tilde{g}_r = 10^{-2}$. Generally, it is shown that the convergent propagation as shown in Figs. 3 and 5 occurs for the negative values of g_i/g_r and $\tilde{g}_i/\tilde{g}_r$, while the divergent propagation as shown in Figs. 4 and 6 occurs for the positive values of g_i/g_r and $\tilde{g}_i/\tilde{g}_r$. Furthermore, it follows from (18)–(23) and (28)–(35) that the critical propagation occurs for zero values of g_i/g_r and $\tilde{g}_i/\tilde{g}_r$, in which the light beam propagates with constant amplitudes of the undulations of the beam trajectory and the spot size, neither converging nor diverging.

If we roughly compare the propagation behaviors of the light beam in the circularly bent section with those in the straight section, the following becomes clear: in the straight section the undulating trajectory decreases or increases in amplitude with increasing distance z for all cases of (I), (II), and (III), repeating sinusoidal and monotonous oscillations as shown in Figs. 3(a) and 4(a), while in the circularly bent section it exhibits extremely complex oscillations as in Figs. 5(a) and 6(a) except for the case (II) in which the matching conditions for the wavefront coefficient are satisfied. The response of the spot size, however, displays no special difference in the straight and circularly bent sections, as is clear from Figs. 3(b)–6(b).

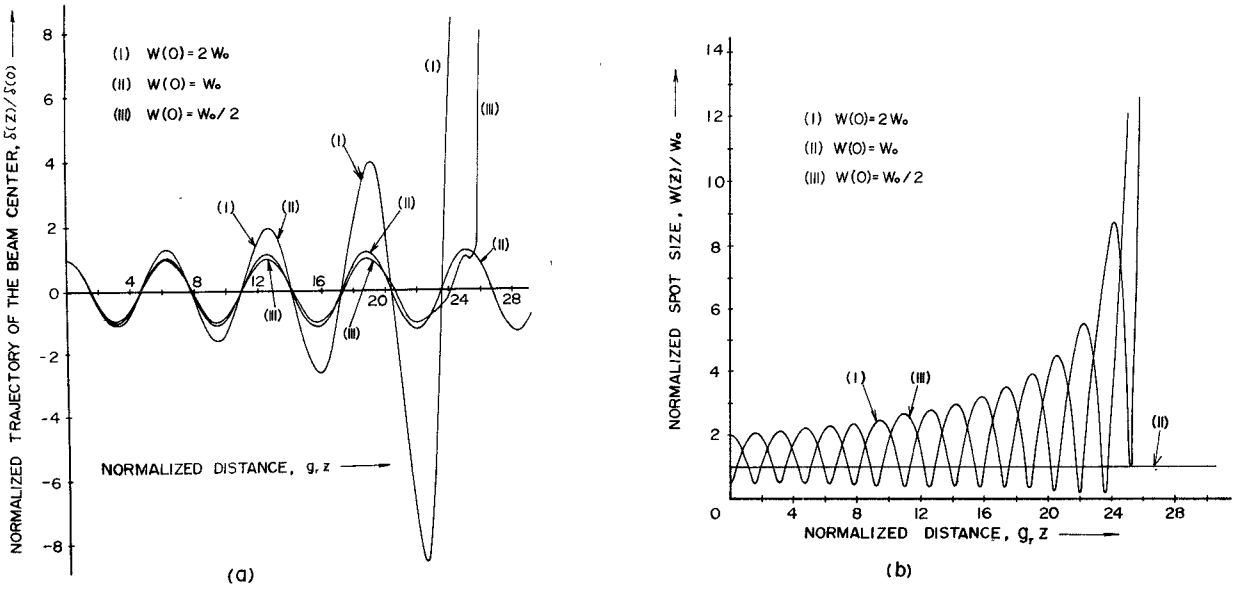

Fig. 4. Propagation behaviors of the divergent light beam guided along the straight section. (a) Normalized trajectory of the beam center. (b) Normalized spot size. ($g_i/g_r = 0.01$, $\epsilon_i/\epsilon_r = 10^{-3}$, $\delta'(0) = 0$, $R(0) = R_0$.)

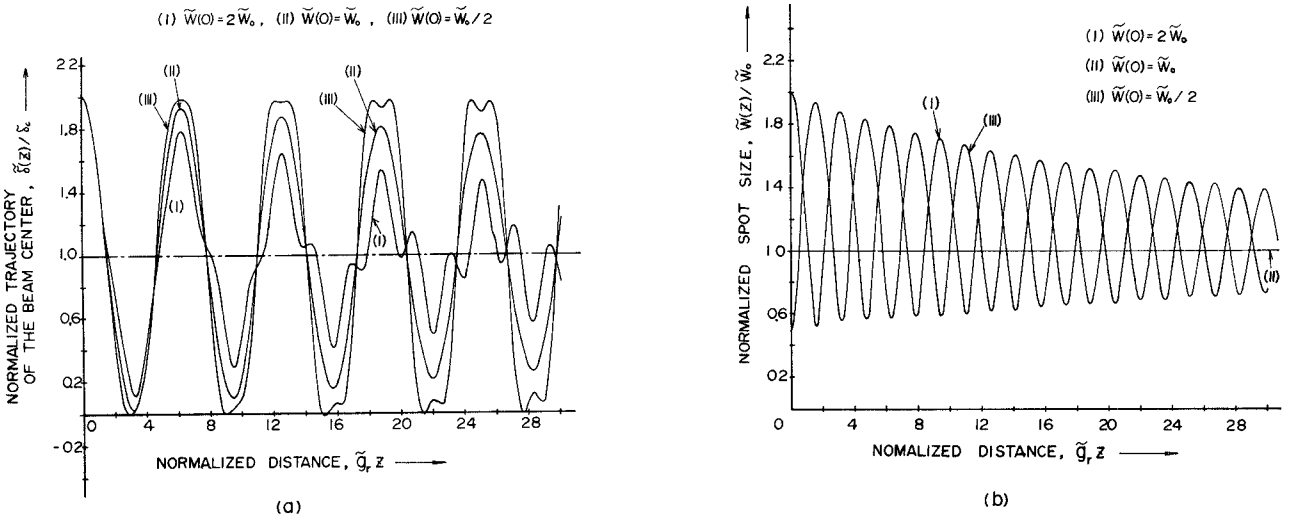

Fig. 5. Propagation behaviors of the convergent light beam guided along the circularly bent section. (a) Normalized trajectory of the beam center. (b) Normalized spot size. ($\tilde{g}_i/\tilde{g}_r = -0.01$, $\epsilon_i/\epsilon_r = 10^{-3}$, $1/\tilde{g}_r R = 0.2$, $\delta'(0) = 0$, $\delta(0) = 2\delta_c$, $R(0) = \tilde{R}_0$.)

D. Physical Explanation of the Convergent, Divergent, and Critical Propagation Behavior

Consider a light beam guided along the straight section of the lens-like medium, the incidence conditions of which are assumed to be arbitrary within paraxial approximations. The light beam can be expressed in terms of an infinite series of normal modes of the medium, Hermite-Gaussian wave beams. The normal modes in the complex-permittivity lens-like medium proceed with the propagation constant γ_n given by (17), whose field intensities vary along the z direction with the function $\exp(-\alpha_n z)$, in which α_n denotes the real part of γ_n

$$\alpha_n \equiv \mathrm{Re}\,\{\gamma_n\} = k_i - (n + \tfrac{1}{2})g_i. \tag{37}$$

Begin with the case of $g_i < 0$. In this case, the second term of (37) is always positive, and hence α_n assumes large positive values for increasing mode number n. Therefore, the more n increases, the more rapidly the function $\exp(-\alpha_n z)$ decreases with increasing values of z. That is to say, the higher order modes decay more rapidly with increasing values of z than the lower order modes. Hence for this case, convergent propagation of the light beam arises as shown in Fig. 3. Contrary to this, for the case of $g_i > 0$, the second term of (37) is negative, so that α_n becomes large in negative values for increasing n. Accordingly, for larger n, $\exp(-\alpha_n z)$ grows more rapidly with increasing z, so that the higher order modes become increasingly dominant as the light beam propagates, which

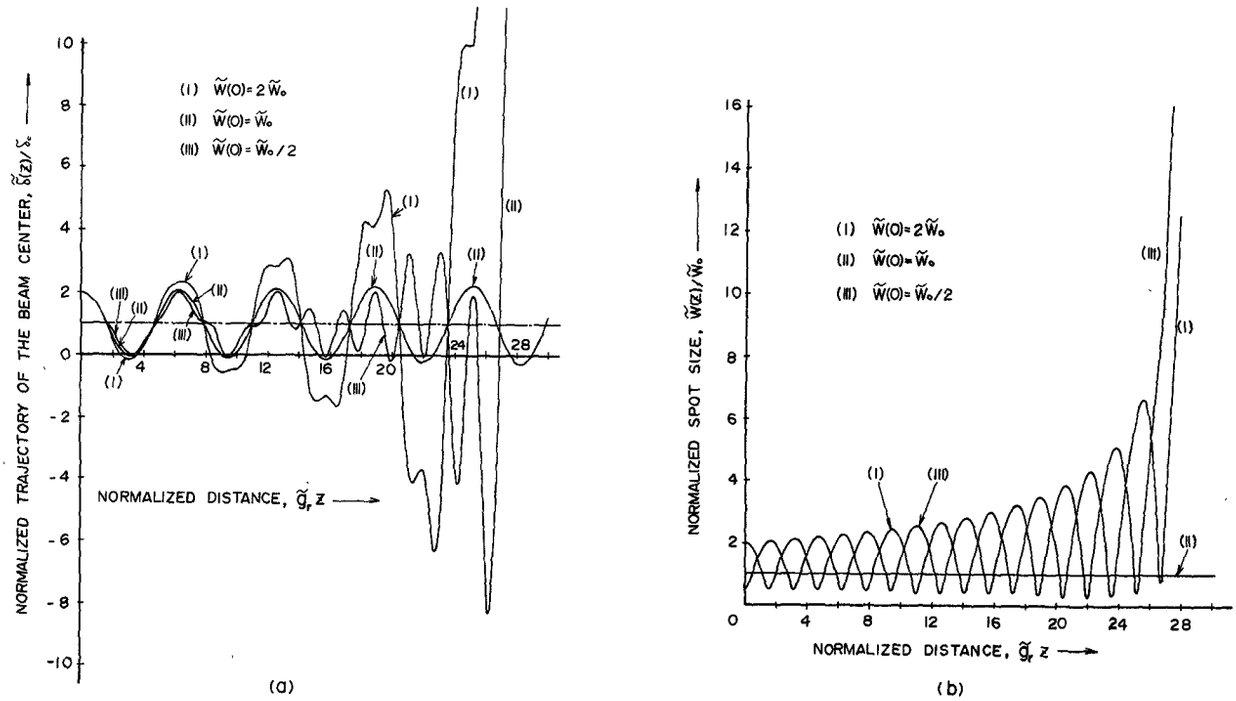

Fig. 6. Propagation behaviors of the divergent light beam guided along the circularly bent section. (a) Normalized trajectory of the beam center. (b) Normalized spot size. ($\tilde{g}_i/\tilde{g}_r = 0.01$, $\epsilon_i/\epsilon_r = 10^{-3}$, $1/\tilde{g}_r R = 0.2$, $\delta'(0) = 0$, $\delta(0) = 2\delta_0$, $R(0) = \tilde{R}_0$.)

causes divergent propagation as illustrated in Fig. 4. On the other hand, for the case of $g_i = 0$, we have $\alpha_n = k_i$ = constant, independent of mode number n, so that $\exp(-\alpha_n z)$ takes the same values for all the normal modes. As a result, the ratio of the normal modes to each other does not vary as the values of z increase, which implies that critical propagation with the constant amplitudes of undulations occurs.

A similar physical explanation is also possible for the propagation behavior of the light beam along the circularly bent section.

E. Relationship between the Complex-Permittivity Profile and the Conditions for the Convergent, Divergent, and Critical Propagations

The conditions for the convergent, divergent, and critical propagations of the light beam $g_i < 0$, $g_i > 0$, and $g_i = 0$ can be rewritten as $\epsilon_r G_i^2 < \epsilon_i G_r^2$, $\epsilon_r G_i^2 > \epsilon_i G_r^2$, and $\epsilon_r G_i^2 = \epsilon_i G_r^2$, respectively, in terms of the medium constants characterizing the complex-permittivity profile. If we introduce new parameters ϵ_ρ and G_ρ^2 defined by $\epsilon_\rho \equiv \epsilon_i/\epsilon_r$ and $G_\rho^2 \equiv G_i^2/G_r^2$, we can illustrate the above conditions in the ϵ_ρ–G_ρ^2 plane as shown in Fig. 7, assuming $\epsilon_r G_r^2 > 0$. The hatched region above the oblique line $G_\rho^2 = \epsilon_\rho$ is the divergent region leading to divergent propagation, while the region below the straight line $G_\rho^2 = \epsilon_\rho$ is the convergent region causing convergent propagation. Moreover, the region on the oblique line $G_\rho^2 = \epsilon_\rho$ is the critical region giving rise to critical propagation. The points $a,b,\cdots,i$ in the same figure correspond to the complex-permittivity profiles as illustrated in Fig. 2(a),(b),(c),$\cdots$,(i), respectively. The points e_1, e_2, e_3, and i_1, i_2, i_3 in Fig. 7 correspond to the profiles (1), (2), (3) in Fig. 2(e) and (i), respectively. The profiles such as Fig. 2(b), (g), (h), and (1) in Fig. 2(e) and (i) belong to the divergent region in Fig. 7 and give rise to the divergent propagation of the light beam as shown in Fig. 4, whereas the profiles such as Fig. 2(c), (d) and (3) in Fig. 2(e) and (i) belong to the convergent region in Fig. 7 and lead to the convergent propagation as shown in Fig. 3. Furthermore, the profiles like (2) in Fig. 2(e) and (i) belong to the critical region, causing the critical propagation in which the light beam propagates with a constant amplitude of undulation.

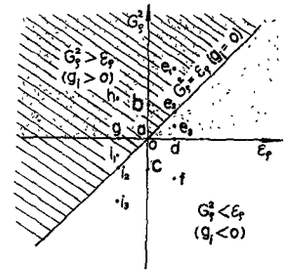

Fig. 7. Convergent region ($G_\rho^2 < \epsilon_\rho$), divergent region ($G_\rho^2 > \epsilon_\rho$) and critical region ($G_\rho^2 = \epsilon_\rho$), assuming that $\epsilon_r G_r^2 > 0$. Diagonal area: divergent region according to the present analysis. Dotted area: divergent region according to the previous analyses [3]–[6].

Converging and diverging behaviors of light beams have already been discussed in the previous papers [3]–[6]. In those papers, however, the parameter corresponding

to g_i used in the present paper (for example, the parameter $\bar{b}_i$ of [6]) is approximated as

$$g_i \doteqdot \pm\{(1/2\epsilon_r)[(G_r^4 + G_i^4)^{1/2} - G_i^2]\}^{1/2} \quad (38)$$

using the assumption $|\epsilon_i| \ll \epsilon_r$, where the upper or lower sign is chosen, depending on whether $G_i^2 \geq 0$ or $G_i^2 < 0$.

Accordingly, the divergent and convergent regions presented in the previous papers [3]–[6] would be represented by the upper half-plane $G_\rho^2 > 0$ and the lower half-plane $G_\rho^2 < 0$ of Fig. 7, respectively, and also the critical region by the abscissa $G_\rho^2 = 0$, disagreeing with the preceding results of the present paper. Consequently, profiles such as Fig. 2(h) and (f), in which both $G_i^2 > 0$ and $\epsilon_i < 0$, or both $G_i^2 < 0$ and $\epsilon_i > 0$, are assumed with $\epsilon_r > 0$ and $G_r^2 > 0$, would belong to the divergent and convergent regions, respectively, agreeing with our results. On the contrary, the profile (3) in Fig. 2(e), in which $G_i^2 > 0$ and $\epsilon_i > 0$ as well as $\epsilon_r > 0$ and $G_r^2 > 0$ are assumed together with $\epsilon_r G_i^2 < \epsilon_i G_r^2$, would belong to the convergent region of Fig. 7, and hence cause divergent propagation, according to the previous analyses [3]–[6]. The result does not agree with the present paper, where a profile like this should lead to convergent propagation, because of the convergent assumption $\epsilon_r G_i^2 < \epsilon_i G_r^2$, as stated before. Furthermore, the profile (1) in Fig. 2(i), in which $G_i^2 < 0$ and $\epsilon_i < 0$ are assumed with $\epsilon_r > 0$ and $G_r^2 > 0$ as well as $\epsilon_r G_i^2 > \epsilon_i G_r^2$, would be regarded as "convergent," if we accepted the conclusion of the previous papers [3]–[6], while according to the present paper such a profile must be regarded as "divergent" because of the assumption $\epsilon_r G_i^2 > \epsilon_i G_r^2$, as described before. Moreover, profiles such as in Fig. 2(d) and (g), in which both $G_i^2 = 0$ and $\epsilon_i > 0$, or both $G_i^2 = 0$ and $\epsilon_i < 0$, are assumed together with $\epsilon_r > 0$ and $G_r^2 > 0$, would be regarded as "critical," if the previous conclusion were applied, whereas according to the present paper the profile as in Fig. 2(d) must be regarded as "convergent," since the convergent condition $\epsilon_r G_i^2 < \epsilon_i G_r^2$ is satisfied with the assumption $G_i^2 = 0$ and $\epsilon_i > 0$, and the profile as shown in Fig. 2(g) must be regarded "divergent," since the divergent condition $\epsilon_r G_i^2 > \epsilon_i G_r^2$ is satisfied with the assumption $G_i^2 = 0$ and $\epsilon_i < 0$.

Thus we must conclude that the previous papers [3]–[6] do not always yield satisfactory results in regard to the criteria for the convergent, divergent, and critical propagation behavior of the light beam along the lens-like medium with complex permittivity.

IV. CONCLUSION

The primary characteristics of the light beam guided along the square-law lens-like medium with loss or gain have been analyzed in more detail theoretically and numerically within the paraxial beam approximations. As a result, the effect of the loss or gain distribution of the medium on the propagation of the light beam has been clarified more completely than in the previous analyses.

The present paper presents useful material not only for the evaluation of the effects of the loss distribution inherent in practical optical fibers consisting of lens-like media, but also for the analysis or synthesis of laser resonators or amplifiers including a loss or gain profile in the transverse cross section [8], [9]. The results of the present paper will also be applicable to the optical image transmission system consisting of lens-like media with a loss or gain variation [10].

APPENDIX
SOLUTION OF THE PARAXIAL WAVE EQUATION (13)

An exact solution of (13) is a light wave with Hermite-Gaussian transverse field distribution. Thus we express the field distribution function in the form

$$U(x,z) = \exp[A(z)x^2 + B(z)x + C(z)] \cdot H_{e_n}[D(z)x + F(z)] \quad (A.1)$$

where $A(z)$, $B(z)$, $C(z)$, $D(z)$, and $F(z)$ are unknown parameters, being functions of z, and $H_{e_n}(X)$ refers to the Hermite polynomial of the nth order, defined as

$$H_{e_n}(X) = n! \sum_{m=0}^{[n/2]} \frac{(-1)^m (2X)^{n-2m}}{m!(n-2m)!} \quad (A.2)$$

with

$$n/2 = \begin{cases} n/2, & \text{for } n = 2,4,6,\cdots \\ (n-1)/2, & \text{for } n = 1,3,5,\cdots. \end{cases}$$

Substitute (A.1) in (13) and use the recurrence relation

$$2(n-1)H_{e_{n-2}}(X) = 2XH_{e_{n-1}}(X) - H_{e_n}(X) \quad (A.3)$$

to eliminate the terms of $H_{e_{n-2}}(X)$. Then we obtain

$$\{\Lambda_1(z)x^2 + \Lambda_2(z)x + \Lambda_3(z)\} \cdot H_{e_n}[D(z)x + F(z)] + \{\Lambda_4(z)x + \Lambda_5(z)\} \cdot H_{e_{n-1}}[D(z)x + F(z)] = 0 \quad (A.4)$$

where $\Lambda_i(z)$ $(i = 1,2,\cdots,5)$ denotes functions of z alone, including $A(z)$, $B(z)$–$F(z)$ and their first derivatives with respect to z.

By rearranging the terms in (A.4) with the help of the expansion of the Hermite polynomials, we can express (A.4) as a descending power series in x. To determine the unknown parameters $A(z)$, $B(z)$–$F(z)$, we compare terms with equal powers of x and have the following set of differential equations:

$$j2k(0)\frac{dA(z)}{dz} = 4A^2(z) - g^2k^2(0)$$

$$j2k(0)\frac{dB(z)}{dz} = 4A(z)B(z)$$

$$j2k(0)\frac{dC(z)}{dz} = B^2(z) + 2A(z) - 2nD^2(z)$$

$$jk(0)\frac{dD(z)}{dz} = 2A(z)D(z) + D^3(z)$$

$$jk(0)\frac{dF(z)}{dz} = B(z)D(z) + F(z)D^2(z). \quad \text{(A.5)}$$

Integrating (A.5), we obtain

$$A(z) = -j\frac{k(0)}{2}\frac{1}{\xi(z)}\frac{d\xi(z)}{dz}$$

$$B(z) = -2A(z)\Delta(z) - jk(0)\frac{d\Delta(z)}{dz}$$

$$C(z) = A(z)\Delta^2(z) + j\frac{k(0)}{2}\Delta(z)\frac{d\Delta(z)}{dz} - (n+\tfrac{1}{2})\ln\xi(z) - n\ln D(z) + K_1$$

$$D(z) = \left(K_2\xi^2(z) + j\frac{2}{k(0)}\xi^2(z)\int\frac{dz}{\xi^2(z)}\right)^{-1/2}$$

$$F(z) = D(z)\{K_3\xi(z) - \Delta(z)\} \quad \text{(A.6)}$$

with

$$\xi(z) = a_1\exp(jgz) + a_2\exp(-jgz)$$
$$\Delta(z) = b_1\exp(jgz) + b_1\exp(-jgz). \quad \text{(A.7)}$$

In the foregoing expressions, a_1, a_2, b_1, b_2, K_1, K_2, and K_3 represent integration constants to be determined from the incidence conditions of the light beam.

For convenience, let the field distribution function of the input light beam $U(x,0)$ be expressed as

$$U(x,0) = \exp\left[-\frac{\{x-\Delta(0)\}^2}{2S^2(0)} - jk(0)\Delta'(0)x\right]\cdot H_{e_n}\left[\frac{x-\Delta(0)}{S(0)}\right] \quad \text{(A.8)}$$

and determine the integration constants and the unknown parameters $A(z)$, $B(z)$–$F(z)$. As a result, we get from (A.1)

$$U(x,z) = \exp\left[A(z)\{x-\Delta(z)\}^2 - jk(0)\Delta'(z)x + j[k(0)/2]\{\Delta(z)\Delta'(z) - \Delta(0)\Delta'(0)\}\right]\cdot\frac{(\cos gz + j[\Omega^2/S^2(0)]\sin gz)^{n/2}}{(\cos gz - j[\Omega^2/S^2(0)]\sin gz)^{(n+2)/2}}\cdot H_{e_n}\left[\frac{x-\Delta(z)}{S(0)\{\cos^2 gz + [\Omega^4/S^4(0)]\sin^2 gz\}^{1/2}}\right] \quad \text{(A.9)}$$

in which

$$\Delta(z) = \Delta(0)\cos gz + \frac{\Delta'(0)}{g}\sin gz \quad \text{(A.10)}$$

$$\Delta'(z) = \frac{d}{dz}\Delta(z) \quad \text{(A.11)}$$

$$A(z) = -\frac{1}{2S^2(0)}\left(\frac{\cos gz - j[S^2(0)/\Omega^2]\sin gz}{\cos gz - j[\Omega^2/S^2(0)]\sin gz}\right) \quad \text{(A.12)}$$

$$\Omega = 1/[gk(0)]^{1/2}. \quad \text{(A.13)}$$

In the above expressions, $1/S^2(0)$ is the input wavefront coefficient of the light beam and $1/\Omega^2$ is the characteristic wavefront coefficient. Furthermore, $\Delta(0)$ and $\Delta'(0)$ are unknown constants to be determined from the input slope $\delta'(0)$ and input displacement $\delta(0)$ of the beam center.

From (A.10), (A.11), and (2)–(4) in the text, we see that $\Delta(z)$ and $\Delta'(z)$ in (A.9) are complex-valued, and hence do not represent the beam trajectory of the light beam $\delta(z)$ and its slope $\delta'(z)$, respectively. To find $\delta(z)$ and $\delta'(z)$, let $\Delta(z)$ and $\Delta'(z)$ be separated into the real and imaginary parts as

$$\Delta(z) = \Delta_r(z) + j\Delta_i(z)$$
$$\Delta'(z) = \Delta_r'(z) + j\Delta_i'(z) \quad \text{(A.14)}$$

and let the sum of the first and second parts of the exponential term in (A.9) be transformed as

$$A(z)\{x-\Delta(z)\}^2 - jk(0)\Delta'(z)x = A(z)\left\{x + \frac{B_r(z)}{2A_r(z)}\right\}^2 - j\frac{x}{A_r(z)}\{A_i(z)B_r(z) - A_r(z)B_i(z)\} + A(z)\left\{\Delta^2(z) - \frac{B_r^2(z)}{4A_r^2(z)}\right\} \quad \text{(A.15)}$$

where $A_r(z)$ and $A_i(z)$ are the real and imaginary parts of $A(z)$, and $B_r(z)$ and $B_i(z)$ represent the real-valued functions as

$$B_r(z) = -2\{A_r(z)A_r(z) - A_i(z)\Delta_i(z)\} + k_r\Delta_i'(z) - k_i\Delta_r'(z)$$
$$B_i(z) = -2\{A_r(z)\Delta_i(z) + A_i(z)\Delta_r(z)\} - k_r\Delta_r'(z) - k_i\Delta_i'(z). \quad \text{(A.16)}$$

From (A.15) and (A.16), we get the expressions for the trajectory of the beam center $\delta(z)$ and its slope $\delta'(z)$ as

$$\delta(z) = -\frac{B_r(z)}{2A_r(z)} = \Delta_r(z) - \frac{A_i(z)}{A_r(z)}\Delta_i(z) + \frac{k_i\Delta_r'(z) - k_r\Delta_i'(z)}{2A_r(z)} \quad \text{(A.17)}$$

$$\delta'(z) = \frac{d}{dz}\delta(z). \quad \text{(A.18)}$$

Puting $z = 0$ in (A.17) and (A.18) yields two equations in two unknowns, $\Delta(0)$ and $\Delta'(0)$. Solving for these un-

knowns, we obtain

$$\Delta(0) = \left\{1 - \frac{k_i S_r^4}{1 + 2k_i S_r^4 Q}\left(\frac{g_i}{\Omega_r^2} + \frac{g_r}{\Omega_i^2}\right)\right\}\delta(0) + \frac{k_i S_r^2}{1 + 2k_i S_r^4 Q}\delta'(0) \quad \text{(A.19)}$$

$$\Delta'(0) = -\frac{S_r}{1 + 2k_i S_r^4 Q}\left(\frac{g_i}{\Omega_r^2} + \frac{g_r}{\Omega_i^2}\right)\delta(0) + \frac{1}{1 + 2k_i S_r^4 Q}\delta'(0) \quad \text{(A.20)}$$

where

$$Q = \frac{\Omega_r^4 \Omega_i^4}{\Omega_r^4 + \Omega_i^4}\left[\frac{1}{S_r^2 S_i^2}\left(\frac{g_r}{\Omega_r^2} + \frac{g_i}{\Omega_i^2}\right) + \frac{1}{2}\left(\frac{1}{S_r^4} - \frac{1}{S_i^4}\right)\left(\frac{g_i}{\Omega_r^2} - \frac{g_r}{\Omega_i^2}\right)\right] \quad \text{(A.21)}$$

with

$$\frac{1}{\Omega_r^2} = \mathrm{Re}\left\{\frac{1}{\Omega^2}\right\}, \qquad \frac{1}{\Omega_i^2} = -\mathrm{Im}\left\{\frac{1}{\Omega^2}\right\}$$

$$\frac{1}{S_r^2} = \mathrm{Re}\left\{\frac{1}{S^2(0)}\right\}, \qquad \frac{1}{S_i^2} = -\mathrm{Im}\left\{\frac{1}{S^2(0)}\right\}. \quad \text{(A.22)}$$

Substituting (A.19) and (A.20) in (A.14), (A.17), and (A.18), we can determine $\delta(z)$ and $\delta'(z)$, and hence from (A.9), the response of Hermite–Gaussian wave beam with the input displacement of the beam center $\delta(0)$ and its slope $\delta'(0)$ as well as the input wavefront coefficient $1/S^2(0)$.

The expressions for the spot size $w(z)$ and the curvature of the phasefront $1/R(z)$ of the Gaussian beam are also derived from the real and imaginary parts of $A(z)$ as

$$w(z) = 1/[-2A_r(z)]^{1/2} \quad \text{(A.23)}$$

$$\frac{1}{R(z)} = \frac{2}{k_r}A_i(z). \quad \text{(A.24)}$$

Lengthy and tedious algebraic manipulations on (A.17), (A.18), (A.23), and (A.24) together with derivations of $A_r(z)$ and $A_i(z)$ from (A.12) lead to the final results, (19), (23), and (24) in the text.

If we assume the incidence conditions $1/S^2(0) = 1/\Omega^2$, $\delta(0) = 0$, and $\delta'(0) = 0$ in (A.9), we have the simplified expression for $U(x,z)$ as

$$U(x,z) = \exp\left[j(n + \tfrac{1}{2})gz - x^2/2\Omega^2\right]\cdot H_{e_n}[x/\Omega]. \quad \text{(A.25)}$$

Substitution into (11) yields

$$V(x,z) = \exp\left[-j\{k(0) - (n + \tfrac{1}{2})g\}z\right] \cdot \exp\left[-\tfrac{1}{2}(x/\Omega)^2\right]H_{e_n}[x/\Omega]. \quad \text{(A.26)}$$

From (A.26), we find the propagation constant of the normal modes in the straight section γ_n as

$$\gamma_n = j\{k(0) - (n + \tfrac{1}{2})g\} = j\{k_r - jk_i - (n + \tfrac{1}{2})(g_r - jg_i)\}. \quad \text{(17)}$$

ACKNOWLEDGMENT

The author wishes to thank Prof. N. Kumagai of Electrical Communication Engineering at Osaka University for his constant encouragement.

REFERENCES

[1] T. Uchida *et al.*, "Optical characteristics of a light-focusing fiber guide and its applications," *IEEE J. Quantum Electron.*, vol. QE-6, pp. 606–612, Oct. 1970.
[2] A. C. S. von Heel, "A new method of transporting optical images without aberration," *Nature*, vol. 173, p. 39, 1954.
[3] H. Kogelnik, "On the propagation of Gaussian beams of light through lens-like media including those with a loss or gain variation," *Appl. Opt.*, vol. 4, pp. 1562–1569, Dec. 1965.
[4] D. Marcuse, "Modes and pseudomodes in dielectric waveguides," *IEEE Trans. Microwave Theory Tech.*, vol. MTT-18, pp. 62–63, Jan. 1970.
[5] ——, *Light Transmission Optics*. New York: Van Nostrand, 1972, pp. 275–282.
[6] Y. Suematsu, T. Shimizu, and T. Kitano, "Beam waves along complex-permittivity lens-like medium," *Trans. Inst. Elec. Commun. Eng.* (Japan), vol. 53-B, pp. 727–734, Dec. 1970.
[7] S. Sawa and N. Kumagai, "A new method of analysis of the waveguide consisting of lens-like medium," *Trans. Inst. Elec. Commun. Eng.* (Japan), vol. 52-B, pp. 624–631, Oct. 1969.
[8] T. Uchida *et al.*, "Continuous oscillation and amplification in light focusing glass lenses," *Jap. J. Appl. Phys.*, vol. 12, pp. 126–134, Jan. 1973.
[9] G. J. Ernst and J. Witteman, "Modes structure of active resonators," *IEEE J. Quantum Electron.*, vol. QE-9, pp. 911–918, Sept. 1973.
[10] K. Iga, S. Hata, Y. Kato, and H. Fukuyo, "Image transmission by an optical system with a lens-like medium," *Jap. J. Appl. Phys.*, vol. 13, pp. 79–86, Jan. 1974.
[11] H. Kogelnik, "Imaging of optical modes-resonators with internal lenses," *Bell Syst. Tech. J.*, vol. 44, pp. 455–494, Mar. 1965.